Multiresolution Hierarchical Shape Models in 3D Subcortical Brain Structures

Juan J. Cerrolaza[1], Noemí Carranza Herrezuelo[2], Arantxa Villanueva[3],
Rafael Cabeza[3], Miguel Angel González Ballester[2],
and Marius George Linguraru[1]

[1] Sheikh Zayed Institute for Pediatric Surgical Innovation,
Children's National Medical Center, Washington DC, USA
{JCerrola,MLingura}@cnmc.com
[2] Alma IT Systems, Barcelona, Spain
{noemi.carranza,miguel.gonzalez}@alma3d.com
[3] Public University of Navarra, Pamplona, Spain
{rcabeza,avilla}@unavarra.es

Abstract. Point Distribution Models (PDM) are one of the most extended methods to characterize the underlying population of set of samples, whose usefulness has been demonstrated in a wide variety of applications, including medical imaging. However, one important issue remains unsolved: the large number of training samples required. This problem becomes critical as the complexity of the problem increases, and the modeling of $3D$ multiobjects/organs represents one of the most challenging cases. Based on the $3D$ wavelet transform, this paper introduces a multiresolution hierarchical variant of PDM (MRH-PDM) able to efficiently characterize the different inter-object relationships, as well as the particular locality of each element separately. The significant advantage of this new method over two previous approaches in terms of accuracy has been successfully verified for the particular case of $3D$ subcortical brain structures.

Keywords: Shape models, wavelets, subcortical brain structures.

1 Introduction

The segmentation and shape analysis of human subcortical structures is of crucial importance in the treatment and study of certain diseases, diagnosis, and patient follow-up [1]. Due to the inherent limitation of traditional bottom-up segmentation methods which only utilize image information, the incorporation of high level knowledge of the target structure has proven highly effective when dealing with image inaccuracies (e.g., partial volume effects, occlusions, image noise or low contrast). An important milestone in top-down approaches was the parametric statistical shape model proposed by Cootes et al. [4]. This technique consists of describing the population statistics from a set of examples by means of point distribution models (PDMs). Despite the high popularity of this technique and its proven utility, PCA-based PDM presents an important limitation: the high dependence on the training set used. This problem becomes more relevant as the dimensionality of the structure increases, being especially critical

when dealing with $3D$ multiobject shapes like the set of subcortical structures. Trying to overcome some of the drawbacks of PDMs, some authors have proposed alternative approaches such as ICA-based shape models [14]. However, the high-dimensionality issue remains a major problem, being necessary to perform a previous dimensionality reduction via PDM. From a different perspective, other authors have shown the utility of incorporating multiresolution analysis by means of the wavelet transform into the PDM framework. Nain et al. [2] presented a multiscale shape representation approach for $3D$ deep brain structures. However, despite the good results obtained and the potential utility its application is limited to isolated volumes, i.e. not taking into account the relationship between different subcortical structures. In particular, the recent work of Cerrolaza et al. [3] presents a hierarchical multiobject segmentation framework to characterize both, the different inter-object relationships and the particular local variations of each single object. However, its application is restricted to planar $2D$ cases. Despite the promising preliminary results, the extension to $3D$ is far from trivial, being precisely in this context where the potential benefits become really necessary.

The aim of this work is to go one step further int the development of new multiresolution hierarchical algorithms overcoming those difficulties involved in the transition to the highly demanding $3D$ multiobject environment. By means of the wavelets transform, we present a robust $3D$ multiresolution hierarchical framework able to efficiently model the relationships between objects, of crucial importance when considering complex anatomical structures such as subcortical brain structures, as well as the peculiarities of each isolated shape in the set.

2   Shape Variation Modeling via PDM

In the context of PDMs [4] a volume is described using a parametric form consisting of a set of 3-dimensional landmarks distributed across the surfaces. For the general case of a shape composed of M single-object structures, the vector form of the i-th training case, $\mathbf{x}_i$, can be defined concatenating the 3 coordinates of the K ($K \in \mathbb{N}$) landmarks. The statistical shape model is then built by Principal Component Analysis (PCA) of the N ($N \in \mathbb{N}$) aligned training shapes. Any instance of the shape space can be approximated by the equation $\mathbf{x} = \overline{\mathbf{x}} + \mathbf{Pb}$, where $\overline{\mathbf{x}}$ is the mean shape, $\mathbf{P}$ is a matrix formed by the eigenvectors, and $\mathbf{b}$ is a vector defining the set of parameters of the statistical shape model. The number of modes of variation, is commonly limited by the size of the training set since in general $N << K$. That is, the capacity of the model to generate new shapes is strongly conditioned by the training set. This limitation of PDM is known as the high-dimension-low-sample-size problem (HDLSS).

3   Multiresolution Hierarchical PDM (MRH-PDM)

The HDLSS issue becomes more relevant as the complexity of the shape to model increases, with the $3D$ multiobject case considered here being one of the

most challenging and interesting problems to solve. Multiresolution analysis has emerged as a powerful strategy to deal with the HDLSS problem. However most of previous approaches consider only single-object structures [7][2]. Reflecting the interactions between objects can help to not only adequately deal with un-defined intermediate regions but also extract the relevant anatomic relationships of potential relevance in the study of human anatomy and certain pathologies. This section presents the MRH-PDM framework and its application to the study of $3D$ multiobject subcortical structures.

3.1   Multiresolution Decomposition of 3D Multiobject Structures

A wavelet decomposition of a signal can be described as a sub-sampling and dif-ferencing step [12]. The vertices of the coarser and the detail part are computed as certain weighted averages and differences of the original vertices, respectively. This operations are represented by the analysis filters $\mathbf{A}$, and $\mathbf{B}$. The construc-tion of these matrices is not trivial since they must be constructed so that the original mesh can be recovered exactly from the low-resolution version and the wavelet coefficients. During this complementary process the coarser version of the polyhedron is refined by subdividing each triangle into four subtriangles by means of additional vertices at edge midpoints. The resulting refined mesh is modified according to the wavelet coefficients previously obtained. These refining and modifying steps are computed by two other filters, $\mathbf{F}$, and $\mathbf{G}$, respectively.

Lounsbery et al. [5] provide a convenient multiresolution framework to obtain the analysis and synthesis filters for meshes with subdivision connectivity. In particular, we define the multiresolution domain using the octahedron as the reference mesh, with a 4-to-1 splitting step, and a lifter butterfly scheme for tri-angular meshes [13]. The method proposed by Praun and Hoppe [6] is employed to parameterize each structure onto an octahedron.

The matrix notation initially proposed in [5] was originally developed for single-objects structures, and a generalization to the multiobject case was pro-posed in [3], though only for the simple $2D$ case. Once the multiresolution decomposition of the constituent objects is performed according to the pro-cess described above, the extension to the $3D$ domain follows as presented be-low. Suppose $\mathbf{x}_j^0$ represents the remeshed version of the original j-th object $\mathbf{x}_j$ $(1 \leq j \leq M)$. The superscript 0 defines the finest level of resolution. Thus, the logarithmic tree two-band wavelet packet can be formulated as follows:

$$\mathbf{x}^r = \mathbf{A}^r \mathbf{x}^{r-1} \tag{1}$$

$$\mathbf{z}^r = \mathbf{B}^r \mathbf{x}^{r-1} \tag{2}$$

$$\mathbf{x}^{r-1} = \mathbf{F}^r \mathbf{x}^r + \mathbf{G}^r \mathbf{z}^r \tag{3}$$

where $\mathbf{z}^r$ is a vector containing the lost details, and r $(r \in \mathbb{N})$ indicates the level of resolution. Applying this filtering process iteratively we create the filter bank illustrated in Fig. 1.
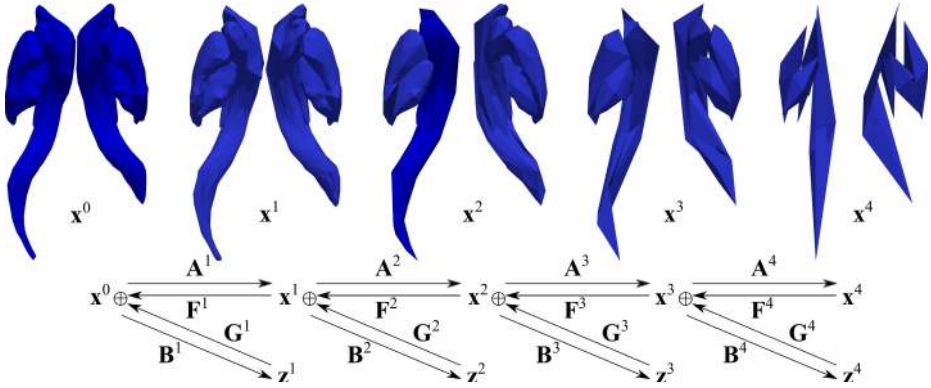
Fig. 1. Schematic representation of a common logarithmic tree 2-band wavelet packet. From left to right fine-to-coarse representations of the subcortical brain structures considered in the paper as they are processed by the wavelet filter bank.

3.2   Description of the Algorithm

With the method described in Section 3.1 it is possible to decompose the multi-object structure into different levels of resolution. This allow us to create specific statistical shape models to characterize different inter-object associations at each scale. Thus, the peculiarities of each single object can be described independently at the finest resolutions, i.e., by means of different PDMs for each object. Then, as we move towards lower levels of resolution it can be appropriate to impose certain spatial restrictions attending to the inter-object relationships by means of more global statistical shape models. In particular a global statistical shape model of the whole set is built at the coarsest resolution in order to guarantee the coherent disposition of the elements. Thus, a specific division of the M objects into M_r disjoint subsets, $(S_1^r, \ldots, S_{M_r}^r)$ is established at each level of resolution. Each of these subsets, S_s^r, where $s = 1, \ldots, M_r$, is formed by the indices of the objects that are modeled jointly at the r-th level of resolution, and therefore: $\bigcap_{s=1}^{M_r} S_s^r = \emptyset$ and $\bigcup_{s=1}^{M_r} S_s^r = (1, \ldots, M)$. An example of hierarchical configuration is depicted in Fig. 2.

Once the multiresolution configuration has been defined, the underlying population of each subset is modeled via PDMs. The step by step description of the process is presented in Fig.3-Alg.1. T_s^r (line Alg.1.11) represents the training set for the s-th subset of objects at the r-th level or resolution, and Λ_s^r (line Alg.1.12) is the set of eigenvalues obtained after applying PCA to T_s^r.

Suppose now we want to describe an image, $\mathbf{y}$, using the new MRH-PDM; i.e., finding the best approximation of $\mathbf{y}$ in the subspace of allowed shapes described by the statistical model. In the context of segmentation algorithms like ASM [4], this procedure is part of an iterative process in which a statistical appearance model guides the matching to a new image (i.e., a new image we want to segment), whereas the statistical shape model guarantees that only plausible instances are generated. Algorithm 2 (Fig. 3-Alg.2) details the hierarchical shape
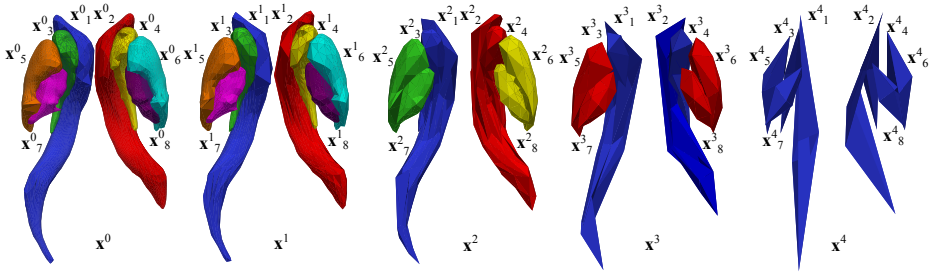
Fig. 2. Example of a hierarchical configuration used to model the inter-object relationships of the eight subcortical brain structures. At each level of resolution, the objects depicted with the same color are modeled jointly via PDM. At the finest resolution ($\mathbf{x}^0$) the left and right lateral ventricles are shown in dark blue and red, caudate nucleus in green and yellow, globus pallidus in light and dark purple, and putamen in orange and light blue, respectively.

Algorithm 1: Hierarchical Statistical Modeling

```
 1 :  {x_(i)}, (i=1,...,N)          ▶ Set of training shapes;
 2 :  for r = 0 to R do
 3 :    for i =1 to N do            ▶ Adapt the resolution
 4 :      if r >0 then                 of each training shape;
 5 :        x^r_(i) = A^r x^{r-1}_(i);
 6 :      else
 7 :        x^0_(i) = x_(i);
 8 :      end if
 9 :    end for
10:    for s = 1 to M_r do         ▶ Create the statistical shape
11:      T^r_s = {x^r_(i),j :j ∈S^r_s,∀i};  model of each subset;
12:      PCA(T^r_s) →{x̄^r_s, P^r_s, t^r_s,Λ^r_s};
13:    end for
14:  end for
```

Algorithm 2: Hierarchical Shape Constraint

```
 1 :  x^0 = y;                       ▶ Adjust the statistical shape model
 2 :  for r = 0 to R do                to the target shape y;
 3 :    if r == 0
 4 :      x̃^0 = x^0;
 5 :    else
 6 :      x̃^r = A^r x̂^{r-1}
 7 :      ẑ^r = B^r x̂^{r-1}
 8 :    end
 9 :    for s = 1 to M^r do
10:      x̃^r_{s} = {x̃^r_j: j ∈ S^r_s};
11:      PDM^r_s(x̃^r_{s}) = x̂^r_{s};  ▶ Use the PDMs built in Algorithm 1
12:    end for                         {x̄^r_s, P^r_s, t^r_s,Λ^r_s}
13:    x̂^r = U^{Mr}_{s=1}x̂^r_{s};
14:  end for
15:  for r = R to 1 do
16:    x̂^{r-1} = F^r x̂^r + G^r ẑ^r;   ▶ Recover the original resolution;
17:  end for
18:  x = x̂^0;
```

Fig. 3. Algorithm 1: Hierarchical statistical modeling. Algorithm 2: Hierarchical shape constraint procedure.

constraint process of $\mathbf{y}$ according to the hierarchical statistical shape model previously built (Fig. 3 -Alg.1). The algorithm applies the corresponding constraints to each subset in which the shape has been divided at each level of resolution, going from the finest to the coarsest level of detail.

4   Results and Discussion

To demonstrate and quantify the performance of this new approach we focus our attention in the particular case of $3D$ subcortical brain structures, though it can be applied in virtually any task involving deformable analysis of complex

Table 1. MRH-PDM Configurations

Res.	Config. 1	Config. 2	Config. 3
$r=0$	$S_1^0=(1); S_2^0=(2); S_3^0=(3); S_4^0=(4); S_5^0=(5); S_6^0=(6); S_7^0=(7); S_8^0=(8)$		
$r=1$	$S_1^1=(1); S_2^1=(2); S_3^1=(3); S_4^1=(4); S_5^1=(5); S_6^1=(6); S_7^1=(7); S_8^1=(8)$		$S_1^1=(1,3); S_2^1=(2,4); S_3^1=(5); S_4^1=(6); S_5^1=(7); S_6^1=(8)$
$r=2$	$S_1^2=(1,3); S_2^2=(2,4); S_3^2=(5,7); S_4^2=(6,8)$	$S_1^2=(1,2); S_2^2=(3,4); S_3^2=(5,6); S_4^2=(7,8)$	$S_1^2=(1,3); S_2^2=(2,4); S_3^2=(5,7); S_4^2=(6,8)$
$r=3$	$S_1^3=(1,2,3,4); S_2^3=(5,6,7,8);$	$S_1^3=(1,2,3,4); S_2^3=(5,6,7,8);$	$S_1^3=(1,3,5,7); S_2^3=(2,4,6,8);$
4	$S_1^4=(1,2,3,4,5,6,7,8)$	$S_1^4=(1,2,3,4,5,6,7,8)$	$S_1^4=(1,2,3,4,5,6,7,8)$

Table 2. Accuracy Evaluation. Landmark-to-landmark errorsd Dice coefficients for the compared methods (PDM, HPDM and MRH-PDM) over eight subcortical structures ($\mathbf{x}_1, \ldots, \mathbf{x}_8$) (see Fig. 2). The last columns shows average results over all the structures.

Point-2-Point Err. (vox.)	$\mathbf{x}_1$	$\mathbf{x}_2$	$\mathbf{x}_3$	$\mathbf{x}_4$	$\mathbf{x}_5$	$\mathbf{x}_6$	$\mathbf{x}_7$	$\mathbf{x}_8$	Avg.
MRH-PDM Config.1	1.48 ± 0.47	1.44 ± 0.53	1.19 ± 0.66	1.20 ± 0.40	$\circ 0.77 \pm 0.16$	$\circ 0.74 \pm 0.12$	$\circ 0.58 \pm 0.12$	$\circ 0.62 \pm 0.18$	$\circ 1.00 \pm 0.51$
MRH-PDM Config.2	$\circ 1.28 \pm 0.50$	$\circ 1.24 \pm 0.49$	$\circ 0.98 \pm 0.48$	$\circ 0.86 \pm 0.37$	$\circ 0.88 \pm 0.18$	$\circ 0.77 \pm 0.20$	0.79 ± 0.21	0.82 ± 0.19	$\circ 0.95 \pm 0.39$
MRH-PDM Config.3	1.48 ± 0.42	1.45 ± 0.53	1.18 ± 0.64	1.20 ± 0.40	$\circ 0.77 \pm 0.17$	$\circ 0.75 \pm 0.11$	$\circ 0.57 \pm 0.12$	$\circ 0.62 \pm 0.18$	$\circ 1.00 \pm 0.50$
HPDM	1.40 ± 0.36	1.40 ± 0.50	1.28 ± 0.67	1.16 ± 0.36	1.06 ± 0.28	0.98 ± 0.24	0.91 ± 0.24	0.93 ± 0.26	1.14 ± 0.43
PDM	1.63 ± 0.41	1.60 ± 0.56	1.30 ± 0.69	1.21 ± 0.39	1.13 ± 0.30	0.97 ± 0.19	0.86 ± 0.24	0.93 ± 0.25	1.20 ± 0.49

Dice Coef.	$\mathbf{x}_1$	$\mathbf{x}_2$	$\mathbf{x}_3$	$\mathbf{x}_4$	$\mathbf{x}_5$	$\mathbf{x}_6$	$\mathbf{x}_7$	$\mathbf{x}_8$	Avg.
MRH-PDM Config.1	0.82 ± 0.04	0.83 ± 0.06	0.86 ± 0.05	0.87 ± 0.04	$\circ 0.93 \pm 0.01$	$\circ 0.93 \pm 0.01$	$\circ 0.93 \pm 0.01$	$\circ 0.93 \pm 0.02$	$\circ 0.89 \pm 0.06$
MRH-PDM Config.2	$\circ 0.84 \pm 0.05$	$\circ 0.85 \pm 0.06$	0.88 ± 0.04	$\circ 0.90 \pm 0.04$	$\circ 0.92 \pm 0.02$	$\circ 0.93 \pm 0.02$	0.91 ± 0.02	0.91 ± 0.02	$\circ 0.90 \pm 0.05$
MRH-PDM Config.3	0.82 ± 0.05	0.83 ± 0.06	0.87 ± 0.05	0.87 ± 0.04	$\circ 0.93 \pm 0.01$	$\circ 0.93 \pm 0.01$	$\circ 0.93 \pm 0.01$	$\circ 0.93 \pm 0.02$	$\circ 0.89 \pm 0.05$
HPDM	0.83 ± 0.05	0.83 ± 0.06	0.87 ± 0.04	0.87 ± 0.04	0.90 ± 0.02	0.91 ± 0.02	0.90 ± 0.03	0.90 ± 0.03	0.87 ± 0.05
PDM	0.80 ± 0.05	0.80 ± 0.07	0.86 ± 0.04	0.86 ± 0.04	0.89 ± 0.02	0.91 ± 0.02	0.91 ± 0.02	0.90 ± 0.03	0.87 ± 0.06

multiobjects volumes. The set of cases to work with are from the Internet Brain Segmentation Repository (IBSR) [8] consisting of 18 T1-weighted volumes, and their manual segmentations of subcortical brain structures (slice thickness 1.5 mm, matrix 256×256 pixels; volumes: $256 \times 256 \times 128$ voxels.). All the volumes are positionally normalized into the Talairach orientation, and processed for bias field correction.

The multiobject shape considered here is composed of eight subcortical structures: left lateral ventricle ($\mathbf{x}_1$), right lateral ventricle ($\mathbf{x}_2$), left caudate nucleus ($\mathbf{x}_3$), right caudate nucleus ($\mathbf{x}_4$), left putamen ($\mathbf{x}_5$), right putamen ($\mathbf{x}_6$), left globus pallidus ($\mathbf{x}_7$) and right globus pallidus ($\mathbf{x}_8$) (see Fig. 2). The meshes of each strucure where registrered through the software Elastix [9] to obtain an adequate set of landmarks. The registration of $3D$ MR data used affine and non-rigid (B-spline transformations and mutual information). After applying the octahedron projection and the remeshing process (Section 3.1), each of the volumes is described by means of 1026 landmarks at the most detailed level of resolution. Since the aim of this study is to evaluate the ability of these different methods to model new instances of the underlying population of shapes, no appearance model is used. Thus, the shape $\mathbf{y}$ in Alg.2 is directly the ground-truth segmentation of the target shape.

To illustrate the performance of the new MRH-PDM we have chosen three different configurations following the general guidelines described in [3] (Table 1). The behavior of the MRH-PDM algorithm is also compared with other two alternative methods: the classical PDM [4], and the hierarchical approach proposed by Davatzikos et al. [7] (HPDM). The average landmark-to-landmark distance

is used as a measure of the accuracy between the results of each method and the ground truth from manual segmentations. We also provide the Dice coefficient as additional error measure. Table 2 shows this information for all the algorithms studied. The leave-one-out approach was used (i.e., 18 different training sets with 17 samples were created, using the remainder case for testing). Compared with the traditional method (PDM), the results show an apparent improvement in accuracy when using either of the two hierarchical methods, HPDM or MRH-PDM. However, this improvement is not significant for HPDM. The mark (°) in Table 2 indicates those cases whose p-value is less than 0.05 when compared HPDM and MRH-PDM with the classical PDM (i.e., the observed improvement over PDM is statistically significant according to the Wilcoxon rank sum test). The mark ($\bullet$) indicates those cases of MRH-PDM with a significant improvement over HPDM. The best results were obtained by configuration 2 of MRH-PDM with an average landmark-to-landmark error of 0.95 ± 0.39 voxels and Dice coefficient of 0.90 ± 0.05, averaged over the subcortical brain structures.

It can be observed that the ventricles in our model are not symmetric in their occipital aspect. This region corresponds to the posterior horns, which are very thin structures barely detectable in MRI, due to partial volume effects. As a consequence, the manual segmentations provided by the IBSR database are not always consistent, as some cases include both posterior horns, while others are missing one or the other. A partial volume estimation technique could be employed to obtain more complete segmentations [11], but we opted for not modifying the ground truth, in order to avoid introducing any bias. This issue suggests an interesting possible extension of our framework: the multi-structure methodology could be adapted to deal with missing structures. The issue of connected substructures is also interesting. Okada et al. [10] propose a method for statistical shape models containing substructures modeled by separate PCA models, while guaranteeing a good connection at the interface. We plan to combine this approach with our multi-resolution $3D$ wavelets framework.

5   Conclusions

In this paper a $3D$ multiresolution hierarchical approach is introduced as alternative to the classical PDM. In cases where multiple objects form a given anatomical region (e.g., the set of subcortical brain structures), the characterization of the relations between subparts provides valuable additional information compared to the single-object modeling approach, i.e., capturing the interaction between adjacent regions in addition to the shape variation of individual regions. This MRH-PDM algorithm allowed to create statistical models to characterize specific inter-object associations at each level of resolution, reducing the HDLSS problem. Though an early and simpler version of this algorithm was recently presented [3], only planar $2D$ cases were considered in that work. However, the HDLSS issue becomes especially pressing as the complexity of the problem increases, being particularly relevant in $3D$ multiobject applications. Thus, the extension to $3D$ becomes necessary in order to obtain real and significant advantages of such approaches for the analysis of medical image data.

The algorithm was compared to two classical approaches, PDM and HPDM. In particular, three different configurations of MRH-PDM were tested, providing significantly better results than the alternative methods, demonstrating the usefulness of incorporating wavelet-based hierarchical approaches to deal with problems of high dimensionality.

References

1. Duay, V., Li, R., DuBois Daische, A., Merchant, T.E., Cmelak, A.J., Donnely, E.F., Niermann, K.J., Macq, B., Dawant, B.M.: Automatic Segmentation of Brain Structures for Radiation Therapy Planning. In: Proc. of SPIE Medical Imaging 2003: Image Processing, pp. 517–526 (2003)
2. Nain, D., Haker, S., Bobick, A., Tannenbaum, A.: Multiscale 3-D Shape Representation and Segmentation Using Spherical Wavelets. IEEE Trans. Med. Imaging 26(4), 598–618 (2007)
3. Cerrolaza, J.J., Villanueva, A., Cabeza, R.: Hierarchical Statistical Shape Models of Multiobject Anatomical Structures: Application to Brain MRI. IEEE Trans. Med. Imaging 31(3), 71–724 (2012)
4. Cootes, T.F., Taylor, C.J., Cooper, D.H., Graham, J.: Active Shape Models Their Training and Application. Comput. Vis. Image Underst. 61(1), 38–59 (1995)
5. Lounsbery, M., DeRose, T.D., Warren, J.: Multiresolution Analysis for Surfaces of Arbitrary Topological Type. ACM Trans. Graph. 16(1), 34–73 (1997)
6. Praun, E., Hoppe, H.: Spherical Parametrization and Remeshing. ACM Trans. Graph. (SIGGRAPH) 22(3), 340–349 (2003)
7. Davatzikos, C., Tao, X., Shen, D.: Hierarchical Active Shape Models, Using the Wavelet Transform. IEEE Trans. Med. Imag. 22(3), 414–423 (2003)
8. IBSR. The Internet Brain Segmentation Repository (IBSR),
   `http://www.cma.mgh.harvard.edu/ibsr/`
9. Klein, S., Staring, M., Murphy, K., Viergever, M.A., Pluim, J.P.W.: Elastix: A Toolbox for Intensity Based Medical Image Registration. IEEE Trans. Med. Imaging 29(1), 196–205 (2010)
10. Okada, T., Linguraru, M.G., Yoshida, Y., Hori, M., Summers, R.M., Chen, Y.-W., Tomiyama, N., Sato, Y.: Abdominal Multi-Organ Segmentation of CT Images Based on Hierarchical Spatial Modeling of Organ Interrelations. In: Yoshida, H., Sakas, G., Linguraru, M.G. (eds.) Abdominal Imaging 2011. LNCS, vol. 7029, pp. 173–180. Springer, Heidelberg (2012)
11. Gonzalez Ballester, M.A., Zisserman, A.P., Brady, M.: Estimation of the Partial Volume Effect in MRI. Medical Image Analysis 6(4), 389–405 (2002)
12. Daubechies, I.: Ten Lectures on Wavelets. Soc. for Industrial and Applied Math., Philadelphia (1992)
13. Dyn, N., Levine, D., Gregory, J.A.: A Butterfly Subdivision Scheme for Surface Interpolation with Tension Control. ACM Trans. Graph. 9(2), 160–169 (1990)
14. Uzumcu, M., Frangi, A.F., Reiber, J.H., Lelieveldt, P.F.: Independent Component Analysis in Statistical Shape Models. In: Proc. of SPIE, pp. 375–383 (2003)